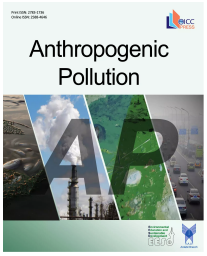

Volume 8, Issue 2, 082423 (1-16)

Anthropogenic Pollution (AP)

https://doi.org/10.57647/j.jap.2024.0802.23

A study on climate change impacts using lumped versus distributed hydrological models in a semi-arid basin

Farahnaz Baharvand[1], Ali Reza Massah Bavani[2], Mohammad Mahdavi[3], Massoud Goodarzi[4,*], Baharak Motamed Vaziri[1]

[1]*Department of Watershed Management, Science and Research Branch, Islamic Azad University, Tehran, Iran.*
[2]*Department of Irrigation and Drainage Engineering, Aburaihan Campus, University of Tehran, Pakdasht, Tehran, Iran.*
[3]*Department of Fisheries, North Tehran Branch, Islamic Azad University, Tehran, Iran.*
[4]*Department of Drought and Climate Change, Soil Conservation and Watershed Management Research Institute (SCWMRI), Agricultural Research, Education and Extension Organization (AREEO), Tehran, Iran.*

[*]**Corresponding author:** massoudgoodarzi@yahoo.com

Original Research

Received:
24 July 2024
Revised:
1 September 2024
Accepted:
8 September 2024
Published online:
15 December 2024

Abstract:

This paper, aims to evaluate the impacts of potential climate change on the stream flow of a semi-arid catchment (called Merek) in western Iran using Distributed Catchment Scale Model (DiCaSM) and IHACRES lumped model and compare their ability in simulation of the future stream flow in this area. The joint probability plot was used to generate seasonal climatic change factors (% change in rainfall and change in temperature °C) to apply as an input to the DiCaSM model. A suite of 15 Atmosphere-Ocean Global Circulation Models (AOGCMs) from the Coupled Model Inter-comparison Project (CMIP) with monthly rainfall and temperature data for the baseline period were evaluated. By analyzing the models, finally, the three best models, including GFDL-CM3, CNRM-CM5 and NorESM1-M models, which reproduce the climatic behavior of monthly temperature and precipitation values, were selected. To study the impact of future climatic change on water supply, this study applied the RCP Scenarios. It proved an acceptable performance in reproducing of the historical observations three Representative Concentration Pathways (RCP2.6, RCP4.5, and RCP8.5) scenarios for the future period $2040-2069$. Results indicated that both hydrological models were able to simulate the observed stream flow successfully in the study catchment. The projections of three AOGCMs showed that the future temperature would be increased in the area, while there was no agreement between the models in simulation of future rainfall. Changes in stream flow simulated by DiCaSM model were ranged from -5.2% to 6.2% for the period $2040-2069$, while for IHACRES model, the changes ranged from -37.7% to 10.1%. Overally the model performed extremely well for both the calibration and validation years. It is recommended to use these hydrological models for a general evaluation of climate change impact in water resources studies.

Keywords: Climate change; DiCaSM; IHACRES; RCP scenarios; Stream flow

1. Introduction

Global climate change refers to a change in the mean climate conditions lasting for several decades or longer. This includes changes in weather conditions of the earth such as global temperature in addition to changes in the frequency of heat waves, droughts, floods, storms, and other extreme weather events in different regions (Adedeji et al., 2014). Climate changes such as changes in temperature, precipitation, intensity-duration-frequency of rainfall events, or other climatic variables can potentially affect water resources (Aghbolagh and Fataei, 2016). The projected impacts of climate change in the future can further exacerbate the current status of water deficit in arid and semi-arid regions. These regions can probably experience more severe and frequent

droughts, complicating water management in the future (Otagvar et al., 2024). The ecosystems of arid and semi-arid regions are highly vulnerable and sensitive. Severe droughts can have huge impacts on agriculture, household users, industry, and tourism (Kahil et al., 2015).

The effective management of future water resources is essential, which requires appropriate supportive decision-making systems including modelling tools. Modeling approaches have widely been used for over 40 years, but most of them have been mainly developed to be used in humid regions. Despite the importance of water in arid and semi-arid regions, the main limitation in hydrologic development of these regions is the lack of high-quality and high-quantity observations. In semi-arid catchments, mainly in developing countries, it is not possible to use an extensive monitoring program or long-term data recording due to its high costs (Montenegro and Ragab, 2012). For this purpose, we requires a realistic prediction of the future climate using climate change scenarios combined with hydrological models which are relatively reliable under climate change patterns (Dakhlaoui et al., 2017). The most widely used hydrological models are conceptual models (e.g. IHACRES and HBV) and physically-based models (e.g. SWAT and VIC) (Dakhlaoui et al., 2017; Wu et al., 2017). Each of them has their own advantages. Conceptual models are calibrated more easily and require fewer inputs, while, physically-based models provide more details of the hydrological cycle at different spatial scales. Lumped models use a more conceptual representation of the rainfall-runoff processes, while distributed models are physically-based in terms of rainfall-runoff processes (Tarboton, 2003). Lumped models consider the whole catchment as a single unit, while distributed models divide the catchment into sub-units (grid cells). A considerable limitation of lumped models is that their parameters do not vary spatially over the whole catchment and thus, the catchment's hydrological response is evaluated only at the outlet, without considering individual sub-catchments. The parameters of distributed models vary spatially at a resolution determined usually by the user; e.g. land-use, and soil properties (Cunderlik, 2003; Gosling et al., 2011).

Numerous studies have attempted to evaluate the impact of climate changes on the hydrological regime of various catchments across the world (Ragab and Prudhomme, 2002; Gosling et al., 2011; Tan et al., 2017; Al-Safi and Sarukkalige, 2018). In this regard, lumped models including SIMHYD and GR4J (Li et al., 2013), HRON (Hlavcova et al., 2016), IHACRES (Dakhlaoui et al., 2017), semi-distributed models such as HBV-D, (Menzel and Burger, 2002), and distributed models such as DiCaSM (Ragab et al., 2010; Montenegro and Ragab, 2012) and SWAT (Solaymani and Gosain, 2014; Zhang et al., 2016; Yang et al., 2019) have been employed. There is usually a debate in the hydrological modeling studies on the application of distributed and lumped models for climate change impact assessments. Al-Safi et al. (2019) compared two conceptual-HBV and distributed-BTOPMC models to evaluate the impact of climate change on future runoff in Australian catchments. They found that that the conceptual model performed better than the distributed model in capturing the observed stream flow. Moreover, the performance of the models was relatively compatible in the overall direction of future stream flow change, regardless of the magnitude and incompatible regarding the change in the high and low flows under future climate scenarios. Recommendations based on single model results may be highly uncertain whereas application of multiple models will highlight the different sources of uncertainties in impact projections (Teklesadik et al., 2017; Perra et al., 2018).

A few recent works have considered an ensemble of hydrological models in climate change impact projections. Vansteenkiste et al. (2014) investigated the structure and calibration effects of three lumped and two distributed hydrological models on climate change impact results in Belgium. Their study reported high uncertainty in the hydrological modelling for low flow projections. Dams et al. (2015) assessed the climate change impact on runoff using four physically-based hydrological models (SWAT, PRMS and a semi- and fully distributed version of the WetSpa model) in Belgium. Their results showed that the hydrological model structure introduces a large uncertainty on both the average monthly discharge and the extreme peak and low flow predictions under the climate change scenarios. Teklesadik et al. (2017) compared hydrological impacts of climate change of the Upper Blue Nile basin by applying multiple Atmosphere-Ocean Global Circulation Models (AOGCMs), Representative Concentration Pathway (RCP) scenarios and six hydrological models. Their results clarified that AOGCM structure was the main contributor to uncertainty in mean annual discharge projection followed by the hydrological model structure and RCPs, respectively. They suggested using multiple impact models as well as multiple AOGCMs to provide a more robust assessment of climate change impacts. Faiz et al. (2018) evaluated the perforce of five lumped (NAM, GR4J), semi-distributed (WEAP, HBV), and distributed (SWAT) hydrological models using an ensemble of AOGCMs in Northeastern China. Their results emphasized that hydrological models contribute notably to the variations in the projection of discharge in the selected River Basin. Overall, the above-mentioned studies revealed that the hydrological models with a different structural diversity, different AOGCMs and climate change scenarios, would highlight major sources of uncertainty in climate change impact assessments.

Considering the hydrological characteristics of Iran which is located in arid and semi-arid regions of the world, study on the impacts of climate change in this country is necessary. In addition, due to the high uncertainty in the climate change impact assessments, there is a need for applying and inter-comparison of different models in the hydrological impact studies. The aim of this study is to evaluate the impacts of potential climate change on the stream flow of a semi-arid catchment located in western Iran using a physically-based distributed model (DiCaSM) and a conceptual lumped model (IHACRES) based on the Coupled Model Intercomparison Project Phase 5 (CMIP5) AOGCMs under three RCP emission scenarios. In this study, data from two sources were provided; the first source was ob-

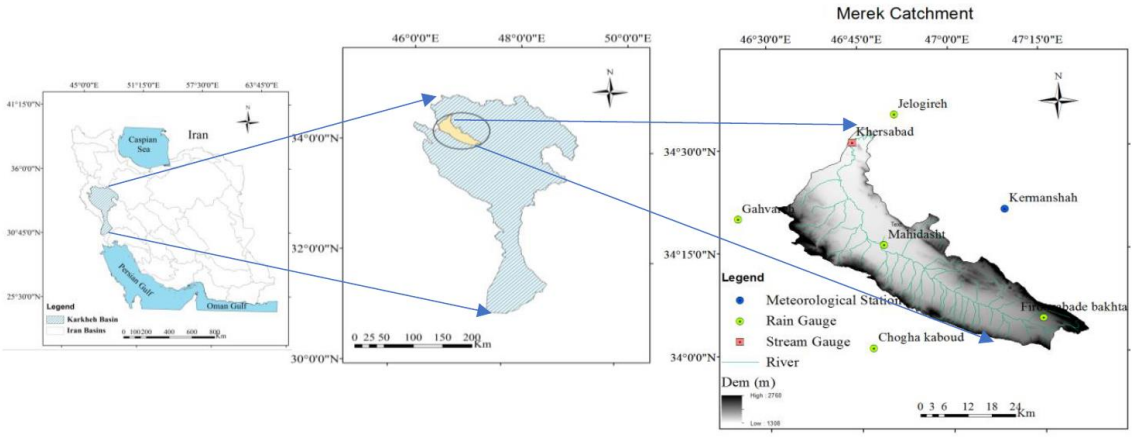

Figure 1. Location of the Merek catchment in Karkheh River Basin, Iran.

served data, which are including hydro-meteorological and geospatial data. These data were used to establish and calibration/validation of the DiCaSM hydrological model. The rainfall and temperature observed data for the period 1971 – 2000 also were used to compare with an ensemble of CMIP5-AOGCMs outputs in the study catchment. The second source was the CMIP5-AOGCMs climatic outputs, which were used to simulate the historical observed data and project the future climate and stream flows under RCP scenarios.

2. Materials and methods

2.1 Study area

The study was conducted in the Merek catchment which is the upper catchment of the Karkheh River Basin in Zagros mountain chains located in western Iran (Fig. 1) whose main drainage is the Merek River. This catchment is a relatively mountainous region with an area of about 1466.15 km^2 and lies between 46°30′-47°23′ E and 34°00′- 34°33′ N. The main river has about 149.5 Km length. The maximum and minimum elevations in the Merek basin are 2760 and 1308 m, respectively, and its mean annual discharge is 1.75 m^3/s. According to Emberger Climate classification, the catchment has a cold and semi-arid climate. Figure 2 shows the annual rainfall of Mahidasht rain gauge located in the catchment from 1971 – 2010. As can be seen, rainfall is varying based on an inter-annual scale which is expected for semi-arid regions. The economy of Mahidasht County is mainly based on agriculture, where hydro-climatic variables are very important.

In this study, the Distributed Catchment-Scale Model, DiCaSM, was used to study the impact of climate change on the hydrology of Merek basin where is a sub-basin of great Karkha Riner Basin(KRB).

2.2 Data

2.2.1 DiCaSM inputs

DiCaSM is the acronym for the Distributed Catchment Scale Model (Bromely and Ragab, 2010; Ragab et al., 2010; Afzal and Ragab, 2019). This model has been developed to estimate the catchment water balance and to account for the impact of the changes in climate and land use on the overall water balance. The DiCaSM model calculates rainfall interception by trees, by the grass and by crops. The infiltration rate, surface run off, groundwater recharge, potential and actual evapotranspiration of mixed vegetation, soil moisture, plant water uptake and stream flow. The model has the option to scale the soil moisture as wetness

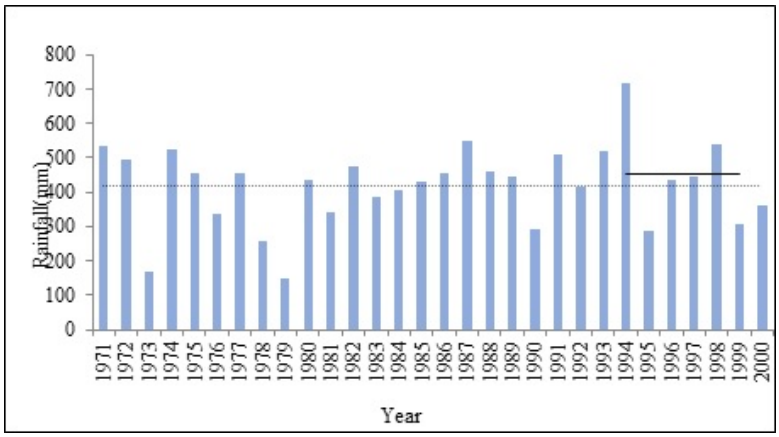

Figure 2. Annual rainfall in the Mahidasht rain gauge during 1971 – 2000.

index. The scaled values range from 0 to 1 for any given day. The value of "1" means the catchment is wet (at maximum soil moisture), while the value of "0" means the catchment is dry (at minimum soil moisture). The Wetness Index WI has the advantage of reducing the spatial variability between different locations. On a certain day, WI can be calculated as:

$$WI = \frac{\sum[(SM_z) - (SM_z)min]}{\sum[(SM_z)max - (SM_z)min]} \quad (1)$$

where SM_z is the soil moisture at depth z, SM_z *max*, and SM_z *min* are the maximum and minimum observed soil moisture at depth z over the simulated/measurement period, respectively. Further details about the equations used in the model are given in Bromely and Ragab (2010). The model calibration is commonly carried out over a short period while the validation period varies from a few years to the entire available record.

The ***DiCaSM*** model requires the following inputs:

• *Daily weather variables*: Including average temperature, sunshine hours, vapor pressure deficit and wind speed. Due to a lack of these meteorological observations in the study catchment, a single meteorological station (Kermanshah) was used which was installed in the catchment area (Fig. 1).

• *Daily rainfall data*: The Merek basin is equipped with some rain gauges; however, only two of them had quantitatively adequate data to be used in this study. Thus, for better spatial results in, data from four other nearby stations were also gathered. Besides, to display the spatial distribution of rainfall, the Thiessen polygon method was applied. The locations of rain gauges are shown in figure 1. Meteorological data were collected from the Iran Meteorological Organization.

• *Land use map*: The map was obtained from the Iranian Agricultural Planning and Economic Research Institute of the Agriculture Ministry. It was double checked and trimmed using field check points before applying in the model (Fig. 3).

• *Digital Elevation Model (DEM)*: A DEM with 50-m resolution was prepared from Soil Conservation and Watershed Management Research Institute (SCWMRI, AREEO) (Fig. 1).

• *Vegetation parameters*: Including leaf area index (LAI), height, canopy resistance, and albedo.

• *Soil series*: Including sand, clay, and silt percentage, organic matter content, and cation exchange capacity for different soil layers. This information was extracted from the pedological information of the region. Moreover, soil properties including saturated hydraulic conductivity, field capacity, and wilting point were predicted using pedotransfer functions (Rawls and Brakensiek, 1989), and the daily discharge data were collected from Khersabad stream gauge located in the outlet of the basin (Fig. 1).

Based on nearest synoptic station to the study area, Kermanshah station, climate is semi-arid and cold. Soil temperature and moist regimes are thermic and xeric respectively. The maximum daily air temperature is 37.7 °C in July and the minimum daily air temperature is -3.8 °C in January. The annual rainfall is about 458 mm (Table 1).

2.2.2 CMIP5-AOGCMs data

The daily climate data required for the model were rainfall, temperature, wind speed, net radiation and actual vapor pressure. The daily observed data were obtained the stations existing in the basin and nearby from Iranian Meteorologic Organization and Water Management Company. As for the coupled models, a suite of 15 CMIP-AOGCMs (Table 2) with available monthly rainfall and temperature data were evaluated for the historical period 1971 – 2000 in the catchment area. The CMIP models include four new greenhouse gas emission scenarios called RCP, which was adopted from the Fifth Assessment Report (AR5) of the Intergovernmental Panel on Climate Change (IPCC). In this study, three

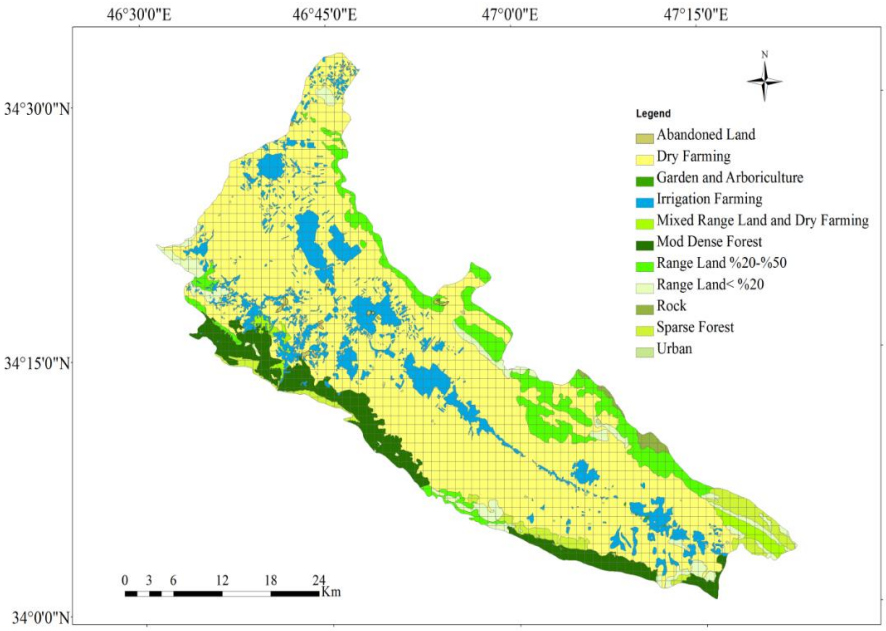

Figure 3. Land use map of the Merek catchment.

Table 1. Climatic data of Kermanshah synoptic station.

Months		Sep.	Oct.	Nov.	Dec.	Jan.	Feb.	Mar.	Apr.	May	Jun.	Jul.	Aug.	Annual Average/sum
TEMP (°C)	Tmax	32.6	24.5	16.4	9.8	6.5	8.7	14	20.2	25.6	33.2	37.7	37	22.2
	Tmin	11.2	6.8	2.3	-0.9	-3.8	-2.7	1.3	5.3	8.8	12.2	16.7	16	6.1
	abs min	6.1	1.4	-4.3	-7.5	-12.8	-10.8	-5.8	-1	3.1	7.4	11.8	11.6	-12.8
	Tmean	21.9	15.7	9.4	4.5	1.4	3	7.5	12.8	17.2	22.7	27.2	26.5	14.1
	Tday	26.6	20.1	13.3	7.6	4.3	6	10	15.8	20.3	26.4	31	30.6	17.7
	Tnight	17	11.8	6.4	2.3	-0.8	0.6	4.7	9.2	13	17.2	21.8	21.4	10.4
Wind speed (m/s) elevation 2m		3.09	3.15	3.26	2.96	3.2	3.36	3.6	3.71	3.49	3.41	3.4	3.2	3.3
relative humidity		22	40	58	71	74	68	61	53	46	27	21	21	46.8
Rainfall (mm)		0.7	32	57.9	81.4	59.8	62.8	84	48.4	29.8	0.8	0.5	0.1	458
Eto		209	141	78.3	45	40	51.8	91	137	185	254	288	265	1784.7
Eto/2		105	70.7	39.2	22.5	20	25.9	45	68.3	92.7	127	144	132	892.2
Day length (hr) (N)		12.2	11.1	10.2	9.7	9.9	10.7	12	12.9	13.8	14.3	14.1	13.3	12
sunshine hours (n)		10.3	7.9	5.9	4	4	5.1	5.7	7	8.2	11.5	11	10.9	7.6

Table 2. The CMIP5-AOGCM models used in the study.

Model	Institution	Grid resolution (long ×lat)
BBC- CSM1.1	Beijing Climate Centre, China Meteorological Administration	2.8125×2.7906
BBC-CSM1.1(m)	Beijing Climate Centre, China Meteorological Administration	2.8125×2.7906
BNU-ESM	College of Global Change and Earth System Science, Beijing Normal University, China	2.8125×2.7906
CanESM2	Canadian Centre for Climate Modelling and Analysis	2.8125×2.7906
CNRM-CM5	Centre National de Recherches Meteorologiques/centre Europeen de Recherche et Formation Avancees en Calul Scientifique, France	1.4062×1.4008
EC-EARTH	European Community Earth System Model	1.125×1.1215
CSIRO-MK3.6.0	Commonwealth Scientific and Industrial Research Organisation in collaboration with the Queensland Climate Change Centre of Excellence, Australia	1.875×1.8653
GFDL-CM3	Geophysical Fluid Dynamics Laboratory, National Oceanic, and Atmospheric Administration (NOAA), United States	2.5×2
GISS-E2-H	NASA Goddard Institute for Space Studies, United States	2.5×2
GISS-E2-R	NASA Goddard Institute for Space Studies, United States	2.5×2
HadGEM2-ES	Met Office Hadley Centre (additional HadGEM2-ES realizations Contributed by instituto Nacional de Pesquisas Espaciais), UK	1.875×1.2
IPSL-CM5A-LR	Institut Pierre-Simon Laplace, France	3.75×1.8947
MPI-ESM-LR	Max Planck Institute for Meteorology, Germany	1.875×1.8653
MPI-ESM-MR	Max Planck Institute for Meteorology, Germany	1.875×1.8653
NorESM1-M	Norwegian Climate centre	2.5×1.8947

scenarios of RCP2.6, RCP4.5, and RCP8.5 were considered to project the future climate change scenarios, where the radiative forcing levels were around 2.6, 4.5, and 8.5 W/m^2, respectively by 2100. The RCP2.6 scenario represents the lowest greenhouse gas emission (Weyant et al., 2009), and RCP8.5 is the highest greenhouse gas emission compared to other scenarios (Vuuren et al., 2011).

2.3 Hydrological models

2.3.1 DiCaSM model

The DiCaSM model is a physically distributed hydrological model developed at the Centre for Ecology and Hydrology in the UK as a part of the MEDIS project by Bromely and Ragab (2010) to study the impact of possible future climate and land-use changes on catchment hydrological processes. The model is used to simulate the hydrology of the unsaturated zone of a catchment area, typically to a depth of a few. DiCaSM is a physically distributed hydrological model and was developed at the Centre for Ecology and Hydrology in the UK as a part of the MEDIS project by Bromely and Ragab (2010) to study the impact of possible future climate and land-use changes on catchment hydrological processes. The model is flexible in its data requirement with different options for the user as it can generate the unmeasured soil hydraulic parameters values from available soil data by pedotransfer functions. The DiCaSM runs at 1 km×1 km grid squares as a default (Bromely and Ragab, 2010); therefore, the study catchment was divided into 1 km^2 cells by using Geographical Information System (GIS) and included 1574 cells. Then, an appropriate dataset was determined for each cell. Figure 4 illustrates the interception process for a cell in DiCaSM model. As can be seen, the main input is "gross

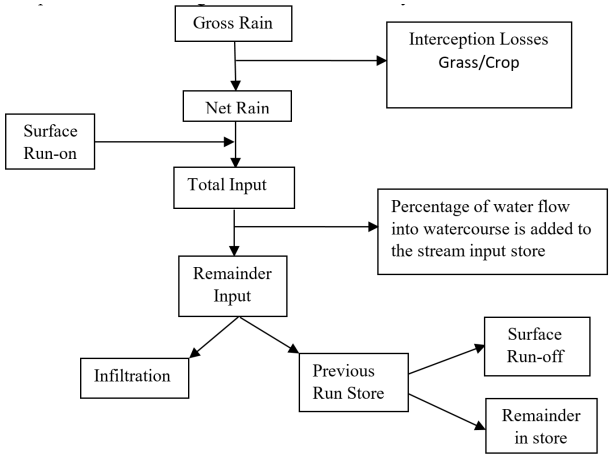

Figure 4. Interception process in DiCaSM model (adapted from the model's User Manual).

rain". The gross rainfall can hit the vegetation present in the cell. The amount of interception by crops and grass was calculated according to approaches applied by Aston (1979) and Hoyningen-Huene (1981), while interception of tress (coniferous/deciduous) was calculated using Gash et al. (1995)'s method. The remained input is "net rain" considered to reach the ground surface of the cell. At this point, another input to the cell was added in the form of "surface run-on" from adjacent cells. The two sources of water were accumulated to provide the "total input"; i.e. the total water that reaches the cell ground surface. At this step, a proportion of water may be taken off as flow into a watercourse if one is already present in the cell. The water that goes to the watercourse is added to the stream input store for the cell. Any water not diverted to the watercourse is referred to as "Remainder Input". The remainder water flow is split split into two parts; some water will infiltrate into the soil and the rest will form surface run-off. As a first step, the model was successfully calibrated and validated for a 41 years period. The DiCaSM model was then used to study the impact of climate change on the water availability.

2.3.2 IHACRES model

The IHACRES model designed by Jakeman et al. (1990) is a conceptual and lumped model that was initially developed for a semi-arid catchment in Australia. The primary goal of the model is to describe the hydrological behavior of the catchment using about six parameters (Littlewood, 2003). This model can be successfully applied in arid and semi-arid regions where the hydrological data is sparse. IHACRES model consists of a non-linear loss module followed by a linear module. The non-linear loss module converts rainfall (r_k) into an effective rainfall (u_k) (Eq. (2)). To obtain the effective rainfall, a catchment wetness index (w_k) is used at each time step:

$$u_k = w_k \times r_k \tag{2}$$

where k is a discrete time step (day); r_k is the rainfall value (mm) at time step k; w_k is the catchment wetness index at time step k, and u_k is the effective rainfall (mm) at time step k. w_k is calculated for each time step based on recent rainfall and temperature data as follows:

$$w_k = c \times r_k + \left(1 - \frac{1}{\tau_w(t_k)}\right) \times w_{k-1} \tag{3}$$

$$\tau_w(t_k) = \tau_w \times e^{0.062 f(R - t_k)} \tag{4}$$

where, τ_w is the catchment drying time constant (day); t_k is the air temperature (°C) at time step k; R shows the reference temperature (°C); f represents the temperature modulation factor (°C^{-1}), and C controls the proportion of rainfall contributing to catchment storage. In the linear routing module, the effective rainfall is converted into stream flow. The routing contains a unit hydrograph (discrete-time linear transfer function). The transfer function includes two parallel storage components; one to show the quick stream flow response and the other to show the slow stream flow response.

2.4 Method

Figure 5 presents a flowchart of the research methodology. It includes the following steps: (a) Evaluation of CMIP-AOGCMs performance in simulating observed data and then selecting appropriate models from among them; (b) Calibration and validation of the hydrological models; (c) Projection of future climate change scenarios, and finally (d) Simulation of future stream flow by the hydrological models under the climate change scenarios.

2.4.1 Evaluation of CMIP5- AOGCM models performance

To evaluate the performance of CMIP-AOGCM models in simulating the observed data, two statistical methods of Root Mean Square Error (RMSE) and the Normalized Standard Deviation (NSD) were used for this study. RMSE is calculated as follows:

$$\mathrm{RMSE} = \sqrt{\frac{\sum_{i=1}^{n}(M_i - O_i)^2}{n}} \tag{5}$$

The NSD is the ratio of standard deviation (SD) of the model to the standard deviation of the observations. It is calculated as follows:

$$\mathrm{NSD} = \frac{SD_{Model}}{SD_{Obs}} = \frac{\sqrt{\frac{\sum_{i=1}^{n}(M_i - \bar{M})^2}{n}}}{\sqrt{\frac{\sum_{i=1}^{n}(O_i - \bar{O})^2}{n}}} \tag{6}$$

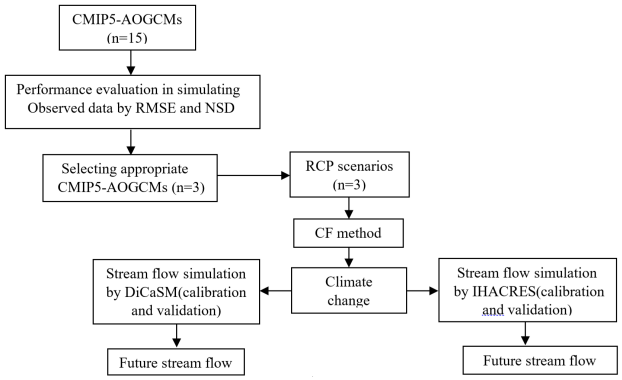

Figure 5. Schematic representation of the study method.

Where, O_i and M_i are the observed and modeled stream flow (m^3/s), respectively, $\bar{O}$ and $\bar{M}$ are the mean observed and modeled stream flow (m^3/s), and n shows the number of samples. The NSD equal to 1 indicates that the observed variability in stream flow is exactly captured by the model, while the NSD value greater or lower than 1 indicates that the model overestimates or underestimates the observed variability (Venkataraman et al., 2016).

2.4.2 DiCaSM calibration and validation

Although the DiCaSM is a physically-based model in terms of hydrological processes, the values of the parameters describing these processes are not global. They vary based on soil, vegetation, and environmental conditions; therefore, calibration of these models against observations is essential. The calibration is performed for the parameters that are of higher importance. Moreover, the model verification was performed to validate the calibrated model parameters for an independent time period The calibration of the DicaSM model is based on a single event (Montenegro and Ragab, 2010; Montenegro and Ragab, 2012; Ragab et al., 2010; Dagostino et al., 2010). Hence, the model was calibrated using a medium-size event in the catchment (February 1991) and then validated for both short period (March 1998) and long period (1997 – 2000).

In this model, the calibration is carried out using an optimization tool. The optimization is based on five key parameters of stream flow. The model provides a calibration against observed data at the outfall of the catchment. The calibration parameters and their values are presented in Table 3. We used an iterative procedure for the optimization where the minimum and maximum values for each of the parameters as well as the number of iterations that should be run between these values are determined. In the end of each iteration, the Nash-Sutcliffe (NS) efficiency coefficient (Nash and Sutcliffe, 1970) is calculated which shows the performance of the model in simulating stream flow. The NS efficiency coefficient shows the goodness-of-fit between the stream flow values derived from the model and those observed. It is calculated as follows:

$$\mathrm{NS} = 1 - \frac{\sum_{i=1}^{n}(O_i - M_i)^2}{\sum_{i=1}^{n}(O_i - \bar{O})^2} \tag{7}$$

where O_i and S_i refer to the observed and simulated river flow data, respectively, and $\bar{O}$ is the mean of the observed data. The NS efficiency ranges from -∞ to 1. The calibration procedure for streamflow consisted of adjusting the six tunable parameters to achieve the best model fit according to the NSE, and the coefficient of determination, R^2. The model performance was also evaluated by using the coefficient of determination and RMSE. R^2 indicates how well the linear regression model fits the observed data. It ranges from 0 to 1. The closer the NS and R^2 values are to 1, the more accurate the model is. R^2 is calculated as follows:

$$R^2 = \left[\frac{n(\sum OM) - (\sum O)(\sum M)}{\sqrt{[n\sum O^2 - (\sum O)^2][n\sum M^2 - (\sum M)^2]}}\right]^2 \tag{8}$$

where O is the observed and M is the modeled stream flow.

Table 3. Values of calibration parameters in DiCaSM model for the Merek catchment.

Parameters	value
Percentage of base flow routed to stream	6%
Exponential function of flow routed to stream	0.00304
Streambed infiltration/leakage percentage	0%
Catchment storage/lag time coefficient	0.215
Stream storage/lag time coefficient	0.656

2.4.3 IHACRES calibration and validation

Calibration of the IHACRES model was based on the parameters of non-linear loss module and linear module described by Jakeman and Hornberger (1994). This model was calibrated for the period 1991 – 1995 based on the daily observed discharge data obtained from the Khersabad stream gauge and validated for the period 1997 – 2000. The significant advantage of these lumped models is that they need only a few input data. The IHACRES model employs daily rainfall and temperature as inputs. Its performance was evaluated using NS efficiency, R^2, and RMSE. The percentage difference in the simulated and the observed flow was minimum.

2.4.4 Downscaling method

In this study, the employed downscaling method for AOGCMs was Change Factor (CF) method. It is a simple and popular method in the climate change studies that makes the output of these models useful for catchment-scale analysis and hydrological modelling (Chen et al., 2011; Diaz-Nieto and Wilby, 2005). In the CF method, the adjustment factors (temperature difference and precipitation ratio predicted by AOGCMs) are calculated by comparing the long-term monthly data for the future and baseline periods. The difference between the future and baseline temperature ($\bar{T}_{AOGCM,fut}$ - $\bar{T}_{AOGCM,base}$) is added to observed temperatures (T_{obs}) (Eq. (9)), and the precipitation ratio ($\frac{\bar{P}_{AOGCM,fut}}{\bar{P}_{AOGCM,base}}$) is multiplied in the observed precipitations (P_{obs}) (Eq. (10)) to obtain the climate change scenarios.

$$T_{fut} = T_{obs} + (\bar{T}_{AOGCM,fut} - \bar{T}_{AOGCM,base}) \tag{9}$$

$$P_{fut} = P_{obs} \times (\frac{\bar{P}_{AOGCM,fut}}{\bar{P}_{AOGCM,base}}) \tag{10}$$

3. Results

3.1 Observed data simulation performance of CMIP5-AOGCMs

Figure 6 illustrates the comparison of the results of 15 CMIP-AOGCM models with the observed temperature and rainfall based on their RMSE and NSD for the historical period 1971 – 2000. Among AOGCM models, GISS-E2-R and GISS-E2-H reported the lowest RMSE of 0.9488 and 1.2464, respectively, and their NSD were almost equal to 1 for temperature simulations (0.9873 for GISS-E2-R and 0.9295 for GISS-E2-H) which indicates that they are more capable of reproducing observed data; however, for rainfall simulations, they showed the highest RMSE (50.6505 and

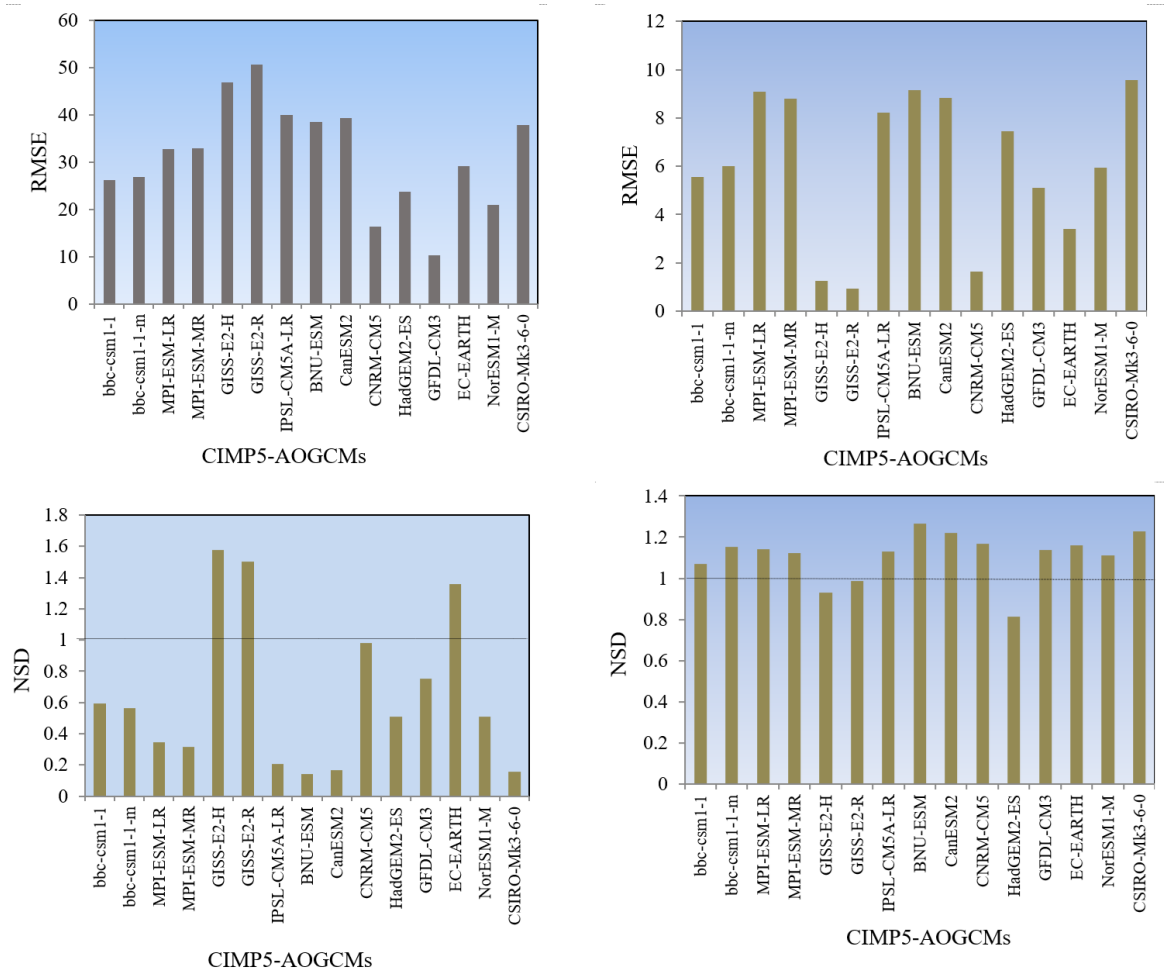

Figure 6. The results of 15 CMIP-AOGCM models with the observed temperature and rainfall.

46.8997, respectively) and their NSD were higher than 1 (1.4998 and 1.5778, respectively). Overall, the comparison of NSD values among all AOGCMs revealed that they all underestimated the observed rainfall except GISS-E2-R, GISS-E2-H, and EC-EARTH which overestimated it. Furthermore, most of the models (except GISS-E2-R, GISS-E2-H, and HadGEM2-ES) overestimated the observed temperature to some extent. According to the RMSE and NSD values, since GFDL-CM3, CNRM-CM5, and NorESM1-M had better results in simulation of monthly rainfall and temperature variations for the period 1971 – 2000, they were selected to investigate the impacts of potential climate change on water resources of the Merek catchment for the future period 2040 – 2069. Overall the model performed extremely well for both the calibration and validation years.

3.2 Calibration and validation of hydrological models

3.2.1 DiCaSM model

For the model calibration, optimization algorithm to identify the best set of parameters has been used. There are six key model parameters that significantly affect the streamflow. These parameters are the percentage of flow routed to stream, catchment storage/time lag coefficient, base flow coefficient, exponent function to describe the peak flow, stream storage/time lag coefficient and stream bed infiltration/leakage. The calibration process involves running an optimization procedure which is based on a simple iteration algorithm in which each of the six optimization parameters were assigned maximum and minimum values. The whole iteration process was carried out using the number of steps between maximum and minimum values of each parameter. The model calculates the Nash-Sutcliffe efficiency value, NSE, the ln NSE, the coefficient of determination, R^2, the total water volume simulated, and total volume observed for the simulated period. The benefit of running the iteration process is to find the best combined values of the six parameters that provide the maximum NSE value.

As mentioned before, calibration and validation of the DiCaSM model were performed using the observed discharge data from Khersabad stream gauge. The calibration was performed for a medium-size event in the catchment (February 1991). Table 4 presents the results of NS efficiency, R^2, and RMSE for the calibration and validation phases, and figure 7 illustrates the DiCaSM calibration for the Merek catchment. An NS efficiency coefficient of 0.95 was obtained for the calibration phase, indicating a good agreement between the simulated and observed values. Figures 8 and 9 illustrate the validation of model for both short (March 1998) and long periods which included low, medium, and high stream flow.

Table 4. DiCaSM calibration and validation statistics for the Merek catchment.

Period	NS (%)	R^2	RMSE	Simulation phase
24.02.1991-01.03.1991	95	0.98	0.51	Calibration
13.03.1998- 21.03.1998	68.12	0.97	10.72	Validation
01.01.1997-31.12.2000	56.70	0.79	2.13	Validation

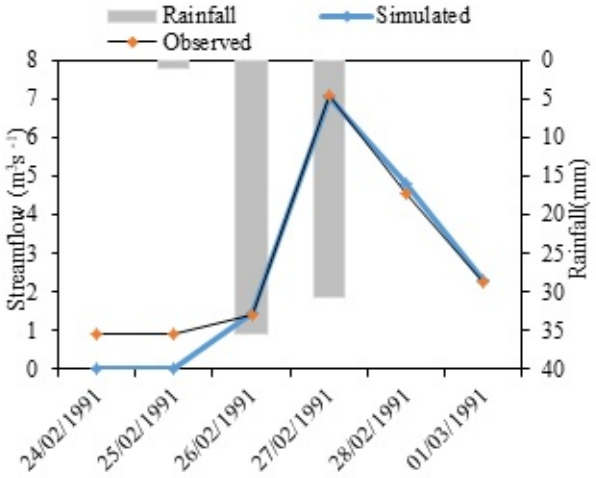

Figure 7. DiCaSM calibration for the event of 1991.

The NS efficiency values of 0.68 and 0.57 were obtained for the short and long periods, respectively. The model tended to underestimate the observed data in the catchment especially for the events exhibiting high stream flow rates resulted in the reduction of NS efficiency in the validation phase; however, the DiCaSM model was capable of reproducing the stream flow observed data and the simulation of short-term and long-term hydrological variations in the study area.

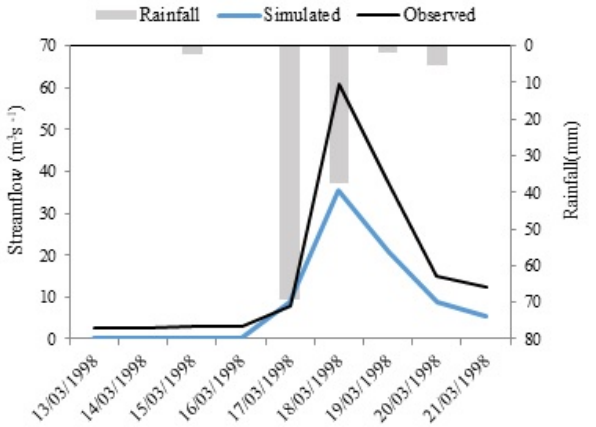

Figure 8. DiCaSM validation for the event of 1998.

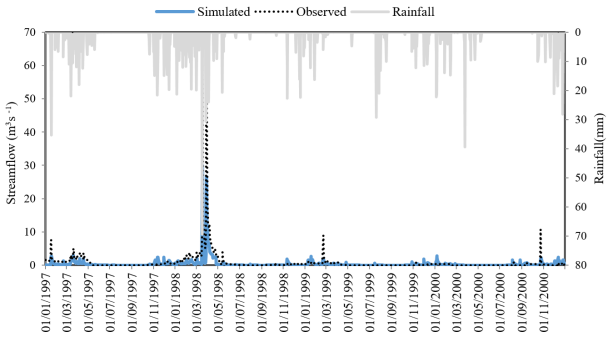

Figure 9. Observed and DiCaSM-simulated stream flow during the validation period 1997 – 2000.

3.2.2 IHACRES model

Several statistical indices were used as model performance indicators to evaluate the goodness of fit and compare the simulated and observed streamflow data. This study applied the Nash–Sutcliffe Efficiency (NSE) coefficient (Nash and Sutcliffe, 1970), as this is the most widely used coefficient to assess the performance of hydrological models (Singh et al., 2010).

Table 5 presents the results of NS, R^2, and RMSE for both calibration and validation phases of simulation for the IHACRES model. The model was calibrated for a long period (1991 – 1995) based on the daily discharge observed data obtained from the Khersabad stream gauge (Fig. 10). The model with the NS efficiency of 0.78 was capable of reproducing the observed stream flow. The model under-

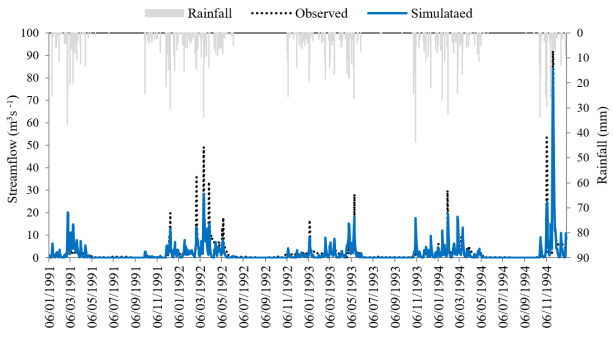

Figure 10. Observed and IHACRES-simulated streamflow during the calibration period 1991 – 1995.

Table 5. IHACRES calibration and validation statistics for the Merek catchment.

Period	τ_w	f	NS (%)	R^2	RMSE	Simulation phase
06.01.1991-01.01.1995	20	1.5	78.28	0.786	2.49	Calibration
01.01.1997-31.12.2000	20	1.5	62.38	0.749	1.99	Validation

Table 6. Changes in the future rainfall and temperature in Merek catchment.

Climate change scenarios	RCPs	CMIP5-AOGCMs	OCT-MAR		APR-SEP	
			Rainfall (%)	Temperature (°C)	Rainfall (%)	Temperature (°C)
CC1	RCP2.6	GFDL-CM3	-15	+3.6	+52	+3.2
CC2	RCP4.5	GFDL-CM3	-17	+3.8	+44	+3.6
CC3	RCP8.5	GFDL-CM3	-24	+5.2	+57	+4.5
CC4	RCP2.6	CNRM-CM5	+15	+1.6	-17	+2
CC5	RCP4.5	CNRM-CM5	+5	+2	-29	+2.5
CC6	RCP8.5	CNRM-CM5	+10	+2.5	-22	+3.4
CC7	RCP2.6	NorESM1-M	-11	+1.6	+20	+1.3
CC8	RCP4.5	NorESM1-M	-10	+1.9	+39	+2.1
CC9	RCP8.5	NorESM1-M	-5	+2.7	+49	+3.1

estimated the observed stream flow data to some extent; however, it showed satisfactory performance in simulating some of the events of high stream flows. The model was validated for the period (Fig. 11). The results of validation confirmed the satisfactory performance of the model in simulating the observed stream flow with an NS efficiency of 0.62.

3.3 Analysis of projected future climate change patterns for the future period 2040 – 2069

Table 6 presents the changes in future rainfall and temperature under different climate change scenarios (CC1 to CC9) for two periods (wet period from October to March, and dry period from April to September). Based on the results, the temperature had an increasing trend under all patterns. According to the GFDL-CM3 and NorESM1-M, the rainfall decreased in the wet period and increased in the dry period under all RCP scenarios, while for the CNRM-CM5, the rainfall increased in the wet period and decreased in the dry period. Figure 12 illustrates the temperature changes in the future period for the three selected AOGCMs relative to the baseline period under climate change scenarios. The GFDL-CM3 generated higher temperature than the other two models.

Figure 13 illustrates the percentage of changes in the rainfall for the future period relative to the baseline period under different climate change scenarios. As can be seen, scenarios CC2, CC3, CC5, and CC 7 show a decrease in rainfall for the future period 2040 – 2069, while scenarios

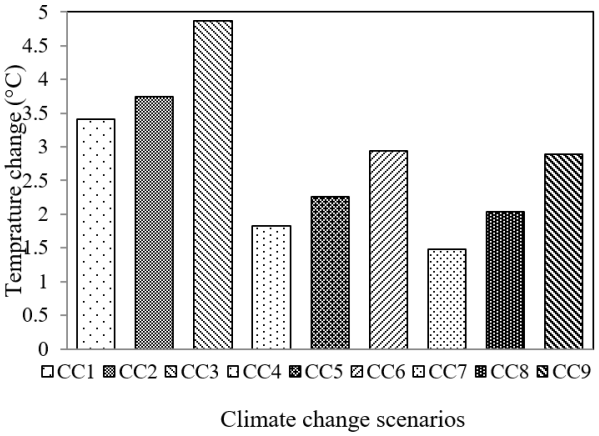

Figure 12. Temperature changes under climate change scenarios in the period 2040 – 2069.

CC1, CC4, CC6, CC8, and CC9 show an increase in rainfall. The CC3 scenario showed the lowest rainfall change (-4.2%), while CC4 and CC9 showed the highest rainfall changes (7 and 7.1%, respectively) among other ones. Table 6 presents the annual changes in temperature and rainfall obtained from the selected CMIP5-AOGCMs for the period 2040 – 2069 under all RCP scenarios. In average, the temperature was projected higher under the RCP8.5 scenario compared to the other two scenarios for all three selected CMIP5-AOGCMs. The future temperature increased by 2.2 °C, 2.6 °C, and 3.5 °C under RCP2.6, RCP4.5, and

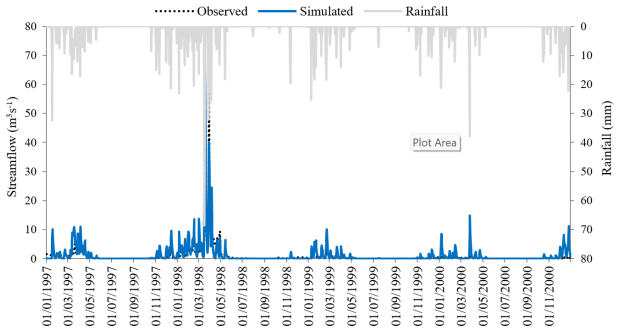

Figure 11. Observed and IHACRES-simulated stream flow during the validation period 1997 – 2000.

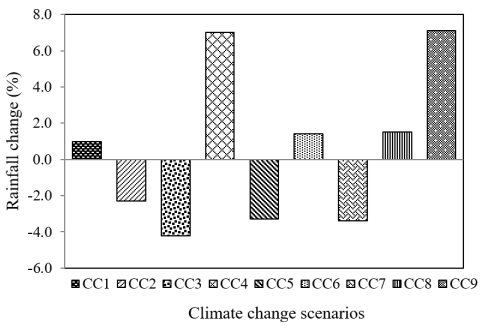

Figure 13. Rainfall changes under climate change scenarios in the period 2040 – 2069.

Table 7. Annual changes in the future rainfall and temperature in Merek catchment.

RCP scenarios	Temperature (°C)				Rainfall (%)			
	GFDL-CM3	CNRM-CM5	NorESM1-M	Avg.	GFDL-CM3	CNRM-CM5	NorESM1-M	Avg.
RCP2.6 (CC1, CC4, CC7)	3.4	1.8	1.5	2.2	1	7	-3.4	1.5
RCP4.5 (CC2, CC5, CC8)	3.7	2.2	2	2.6	-2.3	-3.3	1.5	-1.3
RCP8.5 (CC3, CC6, CC9)	4.9	2.9	2.9	3.5	-4.2	1.4	7.1	1.4

RCP8.5 scenarios, respectively. This future increase can lead to higher evapotranspiration rates and, consequently, decreased soil moisture.

3.4 Future streamflow simulation performance of the study models

3.4.1 DiCaSM model

To analyze the stream flow responses to the future climate changes in the study catchment, the calibrated DiCaSM model for the available climate change scenarios (Table 6) was run separately. Although there is no limitation for running the DiCaSM model in large catchments (Bromely and Ragab, 2010), some studies have focused on using this model in relatively small catchments (e.g. (Dagostino et al., 2010; Montenegro and Ragab, 2010; Montenegro and Ragab, 2012). The model was run by applying the rainfall (%) and temperature (°C) changes in two period of the year (wet and dry) in 2040 – 2069. Table 7 summarizes the future changes in stream flow for the three selected CMIP5-AOGCMs under the three RCP scenarios, and figure 14 illustrates the changes in stream flow under these scenarios. In scenarios CC4 and CC9, the stream flow was projected to increase by 6% and 6.2%, respectively, while in scenarios CC2, CC3, CC5, and CC7, the stream flow tended to decrease by 2.7%, 5.2%, 4.2%, and 4.5%, respectively. The stream flow also showed a slight increase in scenarios CC1, CC6, and CC8.

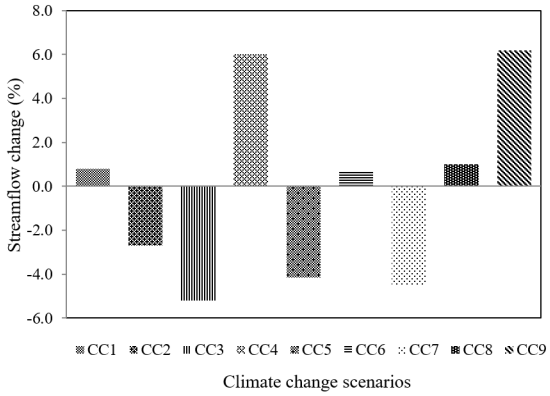

Figure 14. Changes in stream flow simulated by the DiCaSM under climate change scenarios in the period 2040 – 2069.

3.4.2 IHACRES model

Tables 8 and 9 present the results of changes in the stream flow simulated by the calibrated DiCaSM and IHACRES models under three RCP scenarios, and figure 15 illustrates the changes in stream flow under climate change scenarios. As can be seen, the streamflow tends to decrease in all scenarios except in CC4. In comparison with DiCaSM,

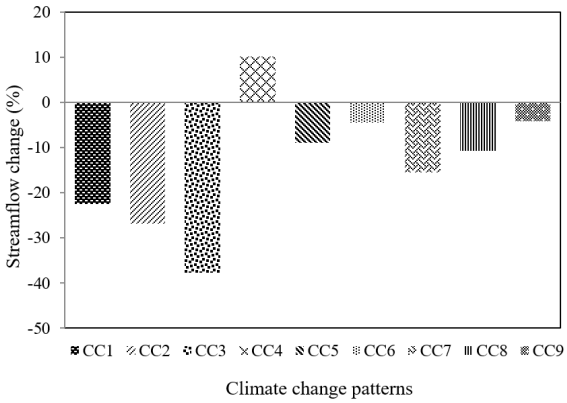

Figure 15. Changes in stream flow simulated by the IHACRES under climate change scenarios in the period 2040 – 2069.

Table 8. Changes in the future stream flow simulated by the DiCaSM model.

RCP scenarios	CMIP5-AOGCMs		
	GFDL-CM3	CNRM-CM5	NorESM1-M
RCP2.6 (CC1, CC4, CC7)	0.8	6	-4.5
RCP4.5 (CC2, CC5, CC8)	-2.7	-4.2	1
RCP8.5 (CC3, CC6, CC9)	-5.2	0.7	6.2

Table 9. Changes in the future stream flow simulated by the IHACRES model.

RCP scenarios	CMIP5-AOGCMs		
	GFDL-CM3	CNRM-CM5	NorESM1-M
RCP2.6 (CC1, CC4, CC7)	-22.5	10.1	-15.5
RCP4.5 (CC2, CC5, CC8)	-26.8	-9	-10.7
RCP8.5 (CC3, CC6, CC9)	-37.7	-4.4	-4.2

IHACRES model had a different behavior in simulating the future stream flow under the same RCP scenarios. This difference was high in GFDL-CM3 and NorESM1-M, while for the CNRM-CM5, it was almost lower.

3.4.3 Model uncertainty analysis

The accuracy of the model results would be clarified with uncertainty analysis. One method for evaluating the uncertainty level is the Generalized Likelihood Uncertainty Estimation (GLUE) which was proposed by **Beven1992<empty citation>** and **Beven2006<empty citation>**. In this study, a detailed uncertainty analysis was conducted and is in the process of separate publication. Thus, the uncertainty analysis will only be briefly highlighted herein. The uncertainty level was evaluated using a number of indicators such the Containing Ratio (**Xiong2009**). CR is the percentage of observed stream flows which are restricted by the prediction bounds (of 5 and 95% likelihood-weighted quantiles). A high CR for the estimated prediction bounds represents a good model fit.

4. Discussion

This study focuses on evaluating the impacts of potential climate change on the stream flow of a semi-arid catchment in western Iran in the mid-21st century. To do this, two lumped (IHACRES) and distributed (DiCaSM) hydrological models were calibrated and validated using discharge data from a stream gauge located in the Merek catchment. The study area suffers from some problems such as overuse of water resources, droughts, limited data, climate variability, and lack of effective water resource management; therefore, our understanding of hydrology in this catchment is of high priority. The DiCaSM model allows the hydrological processes to be simulated per grid cell; hence, it performs across the cells on each day of the runs during a period. Therefore, the model takes longer to run in a large area, but IHACRES is a lumped model that operates at a catchment scale. Overall, the DiCaSM model was able to simulate the historical stream flow in the study catchment. This is consistent with previous studies conducted in other parts of the world on climate change impacts in the semi-arid catchments (e.g. (Montenegro and Ragab, 2010; Montenegro and Ragab, 2012; Ragab et al., 2010; Dagostino et al., 2010). Moreover, the model tended to underestimate stream flows for some small and large events as reported in the studies of Montenegro and Ragab (2010) and Montenegro and Ragab (2012). Such response is expected for semi-arid catchments with limited data (Montenegro and Ragab, 2010). The lack of proper distribution of rain gauges and appropriate data are the factors limiting the description of the real spatial pattern of rainfall over the study catchment. Therefore, this may be attributed to the underestimated stream flow in the catchment. The IHACRES model also performed satisfactorily in simulating the observed stream flow in the study catchment. Overall, it can be stated that, despite the different spatial distribution and hydrological processes, both models had the ability to simulate the daily observed discharge. Simulation of the stream flow should be based on accurately collected data including meteorological observations, hydrological data, multi-period land-use coverage, and soil data (Zhang et al., 2016). However, limited data and field measurements are the main challenges in arid and semi-arid catchments. To study the impacts of future potential climate change on the stream flow of the study catchment, CMIP5-AOGCM models were evaluated by comparing the simulations and historical observations through measuring their RMSE and NSD. The comparisons showed that the GFDL-CM3, CNRM-CM5, and NorESM1-M models had better performance in simulating historical temperature and rainfall in the catchment. To investigate the hydrological changes of the catchment under different climate change scenarios for the future period $2040-2069$, both hydrological models were applied. According to the GFDL-CM3, the stream flow projected by the DiCaSM and IHACRES models under RCP8.5 scenario was lower compared to those under RCP2.6 and RCP4.5 scenarios. According to the CNRM-CM5, the trend of future changes in stream flow was the same under RCP2.6 and RCP4.5 scenarios in both hydrological models. According to the NorESM1-M, the trend of future projected changes in stream flow was the same only under RCP2.6 scenario in two hydrological models. The study hydrological models simulated significantly different stream flow changes under climate change scenarios for the future period. This is consistent with the results of Singh et al. (2010), Zhu et al. (2017) and Faiz et al. (2018) who also compared the response of conceptual-lumped and physically-based distributed hydrological models under future climate changes. According to their results, the model uncertainty affects the hydrological impact of climate change. For example, input data errors are critical in lumped and distributed hydrological modeling in the climate change context. The better understanding of the hydrological models' sensitivity to climate change measured by structured uncertainty analyses, allows better linkage between the simple and complicated models (Jones et al., 2006). Besides, the impact of climate change on the hydrology of catchment somewhat depends on the degree of inherent uncertainty in the AOGCMs processes (Montenegro and Ragab, 2012; Zhang et al., 2016). It is generally difficult to accurately project future climate changes, especially in terms of precipitation; hence, AOGCMs climatic outputs including precipitation and temperature data can introduce uncertainties to future projected stream flow (Zhang et al., 2016). According to the result of this study and others (e.g. (Karlsson et al., 2016; Teklesadik et al., 2017), AOGCMs, the hydrological models with different structures and RCP emission scenarios have major effects on the future climate impact results. Furthermore, the study area, the used approach and the quality of data can influence the projections results (Karlsson et al., 2016; Faiz et al., 2018). Therefore, it is recommended that future studies consider an ensemble of hydrological models with different complexity degree as well as an ensemble of AOGCMs for catchments of Iran to highlight uncertainty sources and further improve the hydrological impact analysis of climate change. Results of the research is aligned with Findings of Afzal and Ragab (2019), Fisher and Rubio (1997), Morris and Flavin (1994).

5. Conclusion

In this paper, the distributed and lumped hydrological models (DiCaSM and IHACRES) and CMIP-AOGCMs were used for the simulation of the future stream flow in the Merek semi-arid catchment. The two hydrological models presented an acceptable performance in simulating the historical stream flow. However, the stream flow simulation results of these models were considerable under future climate change scenarios. The variations in the future stream flow projections of the study catchment depend on the structures and parameters of the hydrological models, CMIP-AOGCMs and the climate change scenarios which can be resulted in high uncertainty in hydrological impacts of climate change. The current study emphasize the application of multiple conceptual and physically-based hydrological models and AOGCMs to improve our knowledge of the hydrological response of semi-arid catchments to the climate change impacts.

Nonetheless, climate models project an increase in evaporation in the summer due to climate change (Wade et al., 2013). This increase in evaporation, combined with greater variations in rainfall between seasons and years will inevitably influence catchment runoff and consequently the water resources. The studied catchment is important because of the land use practices in the area and water abstraction for agriculture, while river flows are low, especially during the summer season. The studied catchment is in the relatively dry western region of Iran. The River is a significant source of the water supply, particularly for agriculture (Khoramnejadian and Fatemi, 2017). This study applied the DiCaSM model (Ragab et al., 2010; Bromely and Ragab, 2010), which has been successfully applied under different climatic conditions, e.g. in the UK (Ragab et al., 2010; Afzal and Ragab, 2019), in Cyprus (Ragab et al., 2010), in the semi-arid region of the northeast of Brazil (Montenegro and Ragab, 2012; Montenegro and Ragab, 2010) and in the south of Italy (Dagostino et al., 2010), not only under climate change scenarios but also applying different possible land use changes. Due to low rainfall for several months, higher water losses due to evapotranspiration, a limited amount of recharge to aquifers and lower runoff of water to rivers. Evapotranspiration is another key component of the hydrological cycle influencing catchment water availability. With a warming atmosphere, an increase in evaporation is expected (Fisher and Rubio, 1997).

Acknowledgments
Authors would like to thank Dr. Ragab (Centre for Ecology and Hydrology, UK) for his valuable and technical assistance in DiCaSM modeling.

Authors contributions
Conceptualization: Alireza Massah Bavani, Mohammad Mahdavi; Data curation: Alireza Massah Bavani, Mohammad Mahdavi; Formal analysis: Farahnaz Baharvand; Funding acquisition: Farahnaz Baharvand; Investigation: Alireza Massah Bavani, Mohammad Mahdavi; Methodology: Alireza Massah Bavani, Massoud Goodarzi; Project Administration: Alireza Massah Bavani, Massoud Goodarzi; Resources: Farahnaz Baharvand; Supervision: Alireza Massah Bavani, Mohammad Mahdavi; Validation: Farahnaz Baharvand; Visualization: Baharak Motamedvaziri; Writing–original draft: Farahnaz Baharvand, Massoud Goodarzi; Writing–review and editing: Massoud Goodarzi

Availability of data and materials
The authors declare that the data supporting the findings of this study are available within the paper.

Conflict of interests
On behalf of all authors, the corresponding author states that there is no conflict of interest.

References

Adedeji O., Reuben O., Olatoye O. (2014) Global Climate Change. *J Geosci Environ Protect* 2:114–122.

Afzal M., Ragab R. (2019) Drought risk under climate and land use changes: implication to water resource availability at catchment scale. *Water* 11:1790. https://doi.org/10.3390/w11091790

Aghbolagh J. Z., Fataei E. (2016) The Studyof Changes in Ardabil Plain Ground Water Level Using GIS. *Advances in Science and Technology Research Journal* 10 (29): 109–115. https://doi.org/10.12913/22998624/61938

Al-Safi H. I. J., Kazemi H., Sarukkalige R. (2019) Comparative study of conceptual versus distributed hydrologic modelling to evaluate the impact of climate change on future runoff in unregulated catchments. *J Water Clim Change*

Al-Safi H. I. J., Sarukkalige P. R. (2018) The application of conceptual modelling to assess the impacts of future climate change on the hydrological response of the Harvey River catchment. *J Hydro-Environ Res.,* https://doi.org/10.1016/j.jher.2018.01.006

Aston A. R. (1979) Rainfall interception by eight small trees. *J Hydrol* 42:383–396. https://doi.org/10.4236/gep.2014.22016

Bromely J., Ragab R. (2010) IHMS-integrated hydrological modelling system. Part1: The hydrological processes and general structure. *Hydrol Process* 24:2663–2680. https://doi.org/10.1002/hyp.7681

Chen J., Brissette F. P., Leconte R. (2011) Uncertainty of downscaling method in quantifying the impact of climate change on hydrology. *J Hydrol* 401:190–202. https://doi.org/10.1016/j.jhydrol.2011.02.020

Cunderlik J. (2003) Hydrologic model selection for the CFCAS Project: Assessment of water resources risk and vulnerability to changing climatic conditions, Project Report I. *University of Western Ontario, Canada.*

Dagostino D. R., Trisorio L. G., Lamaddalena N., Ragab R. (2010) Assessing the results of scenarios of climate and land use changes on the hydrology of an Italian catchment: modelling study. *Hydrol Process* 24:2693–2704. https://doi.org/10.1002/hyp.7765

Dakhlaoui H., Ruelland D., Tramblay Y., Bargaoui Z. (2017) Evaluating the robustness of conceptual rainfall- runoff models under climate variability in northern Tunisia. *J Hydrol* 550:201–217. https://doi.org/10.1016/j.jhydrol.2017.04.032

Dams J., Nossent J., Senbeta T. B., Willems P., Batelaan O. (2015) Multi-model approach to assess the impact of climate change on runoff. *J Hydrol* 529:1601–1616. https://doi.org/10.1016/j.jhydrol.2015.08.023

Diaz-Nieto J., Wilby R. L. (2005) A comparison of statistical downscaling and climate change factor methods: Impacts on low flows in the River Thames, United Kingdom. *Clim Change* 69:245–268. https://doi.org/10.1007/s10584-005-1157-6

Faiz M. A., Liu D., Fu Q., Li M., Baig F., Tahir A. A., Khan M. I., Li T., Cui S. (2018) Performance evaluation of hydrological models using ensemble of General Circulation Models in the north eastern China. *J Hydrol* 565:599–613. https://doi.org/10.3390/w13030299

Fisher A. C., Rubio S. J. (1997) Adjusting to climate change: Implica-tions of increased variability and asymmetric adjustment costs for investment in water reserves. *Environ Econ Manag* 34:207–227. https://doi.org/10.1006/jeem.1997.1011

Gash J. H. C., Lloyd C. R., Lachaud G. (1995) Estimating sparse rainfall interception with an analytical model. *J Hydrol* 170:79–86. https://doi.org/10.1016/0022-1694(95)02697-N

Gosling S. N., Taylor R. G., Arnell N. W., Todd M. C. (2011) A Comparative analysis of projected impacts of climate change on river runoff from global and catchment-scale hydrological models. *Hydrol Earth Syst Sci* 15:279–294. https://doi.org/10.5194/hess-15-279-2011

Hlavcova K., Stefunkova Z., Valent P., Kohnova S., Vyleta R., Szolgay J. (2016) Modelling the climate change impact on monthly runoff in central Slovakia. *Procedia Eng* 161:2127–2132.

Hoyningen-Huene J. Von (1981) Die Interzeption des Niederschlags in Landwirtschaftlichen Pflanzenbestanden. *Arbeitsbericht Deutscher Verband fur Wasserwirtschaft und Kulturbau, DVWK* 57:1–53.

Jakeman A. J., Hornberger G. M. (1994) How much complexity is warranted in a rainfall-runoff model? *Water Resour Res* 29:2637–2649. https://doi.org/10.1029/94WR01804

Jakeman A. J., Littlewood I. G., Withehead P. G. (1990) Computation of the instantaneous unit hydrograph and identifiable component flows with application to two small upland catchments. *J Hydrol* 117:275–300. https://doi.org/10.1016/0022-1694(90)90097-H

Jones R. N., Chiew F. H. S., Boughton W. C., Zhang L. (2006) Estimating the sensitivity of mean annual runoff to climate change using selected hydrological models. *Adv Water Resour* 29:1419–1429. https://doi.org/10.1016/j.advwatres.2005.11.001

Kahil M. T., Dinar A., Albiac J. (2015) Modeling water scarcity and drought for policy adaptation to climate change in arid and semiarid regions. *J Hydrol* 522:95–109. https://doi.org/10.1016/j.jhydrol.2014.12.042

Karlsson I. B., Sonnenborg T. O., Refsgaard J. C., Trolle D., Børgesen C. D., Olesen J. E., Jeppesen E., Jensen K. H. (2016) Combined effects of climate models, hydrological model structures and land use scenarios on hydrological impacts of climate change. *J Hydrol* 535:301–317. https://doi.org/10.1016/j.jhydrol.2016.01.069

Khoramnejadian S., Fatemi F. (2017) Determination of lead and cadmium in the water of the damavand river, Iran. *Appl Ecol Environ Res* 15 (1): 439–444.

Li F., Zhang Y., Xu Z., Teng J., Liu C., Liu W., Mpelasoka F. (2013) The impact of climate change on runoff in the southeastern Tibetan Plateau. *J Hydrol* 505:188–201. https://doi.org/10.1016/j.jhydrol.2013.09.052

Littlewood I. G. (2003) Improved unit hydrograph identification for seven Welsh rivers: implications for estimating continuous streamflow at ungauged sites. *Hydrol Sci J* 48:743–762. https://doi.org/10.1623/hysj.48.5.743.51454

Menzel L., Burger G. (2002) Climate change scenarios and runoff response in the Mulde catchment (Southern Elbe, Germany). *J Hydrol* 267:53–64. https://doi.org/10.1016/S0022-1694(02)00139-7

Montenegro A., Ragab R. (2010) Hydrological response of a Brazilian semi-arid catchment to different land use and climate change scenarios: a modelling study. *Hydrol Process* 24:2705–2723. https://doi.org/10.1002/hyp.7825

Montenegro S., Ragab R. (2012) Impact of possible climate and land use changes in the semi arid regions: A case study from North Eastern Brazil. *J Hydrol* 434-435:55–68. https://doi.org/10.1016/j.jhydrol.2012.02.036

Morris D., Flavin R. (1994) Sub-set of the UK 50 m by 50 m hydro-logical digital terrain model grids. *NERC, Institute of Hydrology, Wallingford*

Nash J. E., Sutcliffe J. V. (1970) River flow forecasting through conceptual models, part I-A discussion of principles. *J Hydrol* 10:282–290. https://doi.org/10.1016/0022-1694(70)90255-6

Otagvar L. Davoodi Memar, Fataei E., Tajiabadi M., Naeimi B. (2024) Spatio-temporal assessment of changes in groundwater quality in Qazvin Plain. *Journal of Range and Watershed Managment* 77 (3): 353–369. https://doi.org/10.22059/jrwm.2024.370962.1744

Perra E., Piras M., Deidda R., Paniconi C., Mascaro G., Vivoni E. R., Cau P., Marras P. A., Ludwig R., Meyer S. (2018) Multimodel assessment of climate change-induced hydrologic impacts for a Mediterranean catchment. *Hydrol Earth Syst Sci* 22:4125–4143. https://doi.org/10.5194/hess-22-4125-2018

Ragab R., Bromley J., Dorflinger G., Katsikides S. (2010) IHMS-integrated hydrological modelling system. Part 2.Application of linked unsaturated, DiCaSM and saturated zone, MODFLOW models on Kouris and Akrotiri catchment in Cyprus. *Hydrol Process* 24:2681–2692. https://doi.org/10.1002/hyp.7682

Ragab R., Prudhomme C. (2002) Climate change and water resources management in arid and semi-arid regions: Prospective and challenges for the 21st century. *Biosyst Eng* 81:3–34. https://doi.org/10.1006/bioe.2001.0013

Rawls W. J., Brakensiek D. L. (1989) Estimation of soil water retention and hydraulic properties. In: Morel-Seytoux HJ (ed) Unsaturated Flow in Hydrologic Modeling: Theory and Practice. *Kluwer Academic Publishers, Netherlands,* 275–300. https://doi.org/10.1007/978-94-009-2352-2-10

Singh C. R., Thompson J. R., French J. R., Kingston D. G., Mackay A. W. (2010) Modelling the impact of prescribed global warming on runoff from headwater catchments of the Irrawaddy River and their implications for the water level regime of Loktak Lake, northeast India. *Hydrol Earth Syst Sci* 14:1745–1765. https://doi.org/10.5194/hess-14-1745-2010

Solaymani H. R., Gosain A. K. (2014) Assessment of climate change impacts in a semi-arid watershed in Iran using reginal climate models. *J Water Clim Change* 6:161–180. https://doi.org/10.2166/wcc.2014.076

Tan M. L., Ibrahim A. L., Yusop Z., Chua V. P., Chan N. W. (2017) Climate change impact under CMIP5 RCP scenarios on water resources of the Kelantan River Basin, Malaysia. *Atmos Res* 189:1–10. https://doi.org/10.1016/j.atmosres.2017.01.008

Tarboton D. G. (2003) Rainfall-Runoff processes, A workbook rainfall-runoff processes web module, chap 6: Simulation of runoff generation in hydrologic models. *Technical Report, Utah State University, Logan, UT, USA*

Teklesadik A. D., Alemayehu T., Griensven A. van, Kumar R., Liersch S., Eisner S., et al. (2017) Inter-model comparison of hydrological impacts of climate change on the Upper Blue Nile basin using ensemble of hydrological models and global climate models. *Clim Change* 141:517–532. https://doi.org/10.1007/s10584-017-1913-4

Vansteenkiste T., Tavakoli M., Ntegeka V., Smedt F. De, Batelaan O., Pereira F., Willems P. (2014) Intercomparison of hydrological model structures and calibration approaches in climate scenario impact projections. *J Hydrol* 519:743–755. https://doi.org/10.1016/j.jhydrol.2014.07.062

Venkataraman K., Tummuri S., Medina A., Perry J. (2016) 21st century drought. Outlook for major climate divisions of Texas based on CMIP5 multimodel ensemble: Implications for water resource management. *J Hydrol* 534:300–316. https://doi.org/10.1016/j.jhydrol.2016.01.001

Vuuren D. P. Van, Edmonds J., Kainuma M., Riahi K., Thomson A., Hibbard K., et al. (2011) The representative concentration pathways: an overview. *Clim Change* 109:5–31. https://doi.org/10.1007/s10584-011-0148-z

Wade S. D., Rance J., Reynard N. (2013) The UK climate change risk assessment: assessing the impacts on water resources to inform policy makers. *Water Resour Manage* 27:1085–1109. https://doi.org/10.1007/s11269-012-0205-z

Weyant J., Azar C., Kainuma M., Kejun J., Nakicenovic N., PR P. R. Shukla, et al. (2009) Report of 2.6 Versus 2.9 Watts/m2 RCPP Evaluation Panel. *Intergovernmental Panel on Climate Change, Geneva, Switzerland,* https://doi.org/10.4081/gh.2016.421

Wu J., Miao C., Zhang X., Yang T., Duan Q. (2017) Detecting the quantitative hydrological response to changes in climate and human activities. *Sci Total Environ* 586:328–337. https://doi.org/10.3390/w14020257

Yang W., Long D., Bai P. (2019) Impact of future land cover and climate changes on runoff in the mostly afforested river basin in North China. *J Hydrol* 570:201–219. https://doi.org/10.1016/j.jhydrol.2018.12.055

Zhang Y., You Q., Chen C., Ge J. (2016) Impact of climate change on stream flows under RCP scenarios: A case study in Xin River Basin, China. *Atmos Res* 178:521–534. https://doi.org/10.1016/j.atmosres.2016.04.018

Zhu D., Das S., Ren Q. (2017) Hydrological appraisal of climate change impacts on the water resources of the Xijiang basin, South China. *Water* 9:793. https://doi.org/10.3390/w9100793